Materials Research, Vol. 1, No. 1, 39-45, 1998.

Effect of Niobium on Corrosion Resistance to Sulfuric Acid of 430 Ferritic Stainless Steel

Neusa Alonso-Falleiros, Stephan Wolynec

Departamento de Engenharia Metalúrgica e de Materiais,

Escola Politécnica da Universidade de São Paulo,

Av. Prof. Mello Moraes, 2463, 05508-900 São Paulo - SP, Brazil;

e-mail: nealonso@usp.br or swolynec@usp.br

Received: April 2, 1998; Revised: July 13, 1998

The influence of niobium on corrosion resistance to 0.5M H_2SO_4 of 17% Cr ferritic stainless steels, to which it was added in amounts larger than that necessary to stabilize the interstitial elements, was investigated. Their performance was compared to that of other two Fe-17%Cr alloys, one without additions and another containing 0.93% molybdenum. Through weight and electrochemical measurements and through morphologic examination of corroded surface it was found that the corrosion of these alloys, with the exception of that containing molybdenum, proceeds in two different steps. In the first step (up to about 60 min) the corrosion rate practically does not change with time, the lower rates being displayed by alloys containing larger amounts of Nb. In the second stage the corrosion rate increases with time. The corrosion rate of Mo containing alloy is constant for all times.

Keywords: *ferritic stainless steel UNS 43000, generalized corrosion, sulfuric acid, niobium additions*

1. Introduction

The ferritic stainless steels display a high corrosion resistance in many environments[1,2]. However, when these steels are cooled from the temperature range 900 °C - 1150 °C, the high diffusion rate of C and N in these alloys determines a fast intergranular precipitation of chromium carbides and nitrides, turning them susceptible to intergranular corrosion[2-6]. One way to overcome this is to lower the C and N content[6,7]. Another alternative is to add a stabilizing element of C and N, such as Nb or Ti, which forms carbides and nitrites preferentially to those of Cr, avoiding thus its intergranular corrosion[2,6,8-12]. This is the main purpose of adding niobium to this type of steels and the amount needed is about eight to eleven times the C plus N content[12].

Another element that has been added to these steels is molybdenum in amounts of 1% to 2%. This element improves considerably their resistance to pitting and crevice corrosion[8,13,14] as well as to generalized corrosion in oxidizing[4] and reducing[1,4] environments.

Effects of other alloying elements in ferritic stainless steels have also been investigated, such as copper[15-17], vanadium[18] and ruthenium[19], but it was found that their effect in increasing the corrosion resistance has not been as significant as that of molybdenum.

Seo *et al.*[17] investigated the effect of niobium on the corrosion resistance of Fe-26Cr ferritic stainless steel in sulfuric acid solution. They found that niobium additions of 0.39 wt% and 0.67 wt% produce a significant enrichment in this element of the steel surface during active dissolution but it is not as effective in suppressing the active dissolution as molybdenum and copper.

The present work is concerned with the effect of niobium on generalized corrosion of 17%Cr ferritic stainless steels in 0.5 M H_2SO_4 solution, when added in amounts larger than those necessary to stabilize the interstitials, the comparison being made with two similar steels, one Nb free and another containing Mo.

2. Experimental

The samples used in this work were obtained from 1.0 kg ingots cast in a vacuum melting furnace. The ingots were

forged at 1200 °C up to a 70% reduction in area, heat treated at 1200 °C during 30 min, water-quenched, heat treated at 800 °C during 90 min and again water-quenched. The treatment at 1200 °C was to fully anneal the material while that at 800 °C was intended to eliminate its sensitization. In this way six different alloys were obtained, whose chemical composition is given in Table 1.

The 0.5 M H_2SO_4 solution was prepared with distilled water and analytical grade chemical. Both the weight loss and the electrochemical tests were performed at 21 ± 1 °C in a naturally aerated solution. Specimens were freshly ground to a 600 grit silicon carbide finish and degreased prior to use.

The corrosion rate was determined by weight loss of 20 mm x 20 mm x 7 mm size specimens using a 0.1 mg precision analytical balance. The specimens were immersed in 500 mL of testing solution contained in a 600 mL beaker, where they were sustained in vertical position with a nylon thread. The necessary care was taken to remove the corrosion products from the surface before the weighing. For each testing time three specimens and a freshly prepared solution were used.

To get a better understanding of the corrosion process the variation of corrosion potential with testing time was also determined. This was performed in a cell containing 700 mL 0.5M H_2SO_4 solution, using 1.0 cm^2 surface area specimens encapsulated in thermosetting plastic. The potential was measured against the saturated calomel reference electrode (SCE) with a potentiostat connected to a x-time recorder.

The morphology of corroded surfaces was examined on the scanning electron microscope (SEM) while the microconstituents were identified by energy dispersion qualitative analysis (EDS).

3. Results

3.1. Weight loss tests

The results of weight loss tests are the averages of three measures performed with each one of the three samples used in each of the testing times. The variation of weight loss with time for alloys 1 (without addition), 2 (with Mo) and 3 (with 0.31% Nb) is shown in Fig. 1. For alloy 1 this variation approaches a curve whose concavity is turned upwards while for alloy 2 it is nearly linear. For alloy 3, on its turn, as well as for other Nb containing alloys (alloys 4, 5 and 6), the curve displays a peculiar behavior. For times up to about 240 min the curve is similar to that of alloy 1, but then the weight loss increase is slowed down, resuming

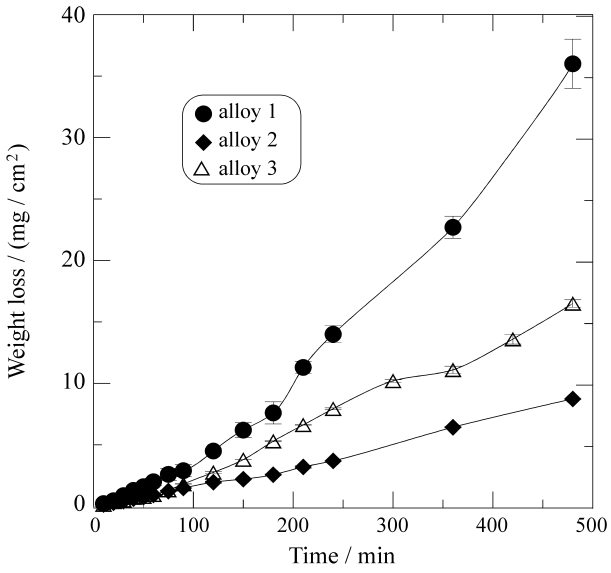

Figure 1. Weight loss as a function of time for alloys 1, 2 and 3 in 0.5 M H_2SO_4. The curves of alloys 4, 5 and 6 are similar to that of alloy 3.

Table 1. Chemical composition of investigated alloys in wt-%.

Element	Alloy					
	1	2	3	4	5	6
C	0.02	0.03	< 0.01	< 0.01	< 0.01	< 0.01
N	0.0062	na	na	na	na	na
Si	0.20	0.13	0.20	0.11	0.11	0.12
Mn	0.21	0.01	0.01	< 0.01	< 0.01	0.02
P	0.02	0.02	0.02	0.02	0.01	0.01
S	0.02	0.02	0.02	0.02	0.02	0.02
Cr	17.2	15.8	16.8	16.5	16.3	16.3
Ni	0.71	1.06	0.73	0.72	0.73	0.70
Mo	-	0.93	-	-	-	-
Nb	-	-	0.31	0.58	1.12	1.62

na = not analyzed.

its original trend at about 400 min. The lack of linearity in the above curves implies that the corrosion rate changes with time.

In order to get further insight about the corrosion behavior of these alloys, the weight loss data was plotted on a log-log graph. Figure 2 gathers the data for alloys 1, 2 and 6 (with 1.62% Nb). It can be noticed that for times larger than 100 min, the Mo bearing alloy (alloy 2) stands out as the most resistant one, the alloy without addition (alloy 1) as the less resistant, while the Nb bearing alloy (alloy 6) displays an intermediate corrosion resistance. The corrosion resistance of other Nb containing alloys (3, 4 and 5) is similar to that of alloy 6.

The dashed line drawn on Fig. 2 indicates the straight line of slope 1.0. It can be observed that the experimental points of alloy 2 fit a straight line parallel to the dashed line, while those of alloys 1 and 6 fit two distinct lines, indicating a two step corrosion process. The remaining Nb bearing alloys (alloys 3, 4 and 5) have a similar behavior. The first line of alloy 1, which holds for times up to 90 min, has a slope slightly larger than that of dashed line. For Nb bearing alloys this line is shorter (it holds for times smaller than 60 min) but its slope is about the same as that of dashed line. The slope of the second step line is considerably larger than that of the dashed line.

The slopes of all lines obtained on the log-log graphs were determined by linear regression and their values together with the respective time range where they hold and the correlation index r^2 are presented on Table 2.

As can be observed in this Table, in the first step the slope values are close to unity, so that it can be assumed that for this time range the weight loss variation is linear with time and the corrosion rate is constant. The values of this rate were also determined by linear regression by fitting a straight line to the weight loss data and they are given in Fig. 3 as a function of Nb content. It can be noticed that in this step the alloy 1 (without addition) has the largest corrosion rate, while the addition of molybdenum (alloy 2) halves this rate. The addition of Nb is even more significant as all four Nb bearing alloys have lower corrosion rates than the Mo bearing alloy, the effect being more marked for increasing Nb contents. The corrosion rate of alloy 6 (1.62% Nb) is more than 30% lower than that of alloy 2 (0.93% Mo).

In the second step the slope assumes values between 1.5 and 1.7, so that the experimental data can fit an equation of the type:

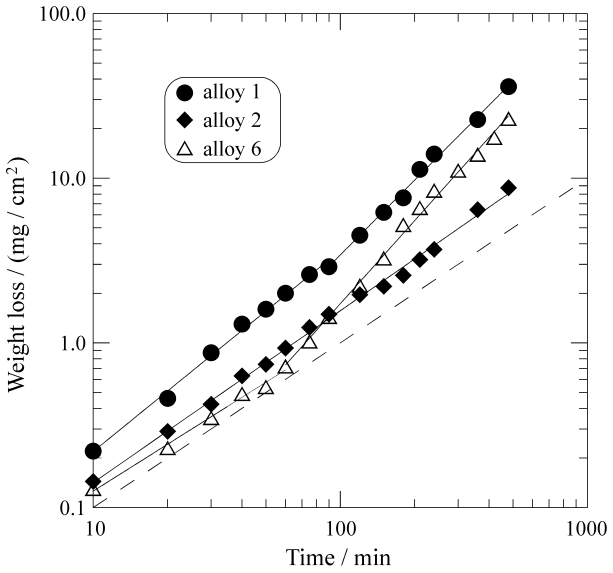

Figure 2. Weight loss as a function of time for alloys 1, 2 and 6 in 0.5 M H_2SO_4 plotted on a log-log graph.

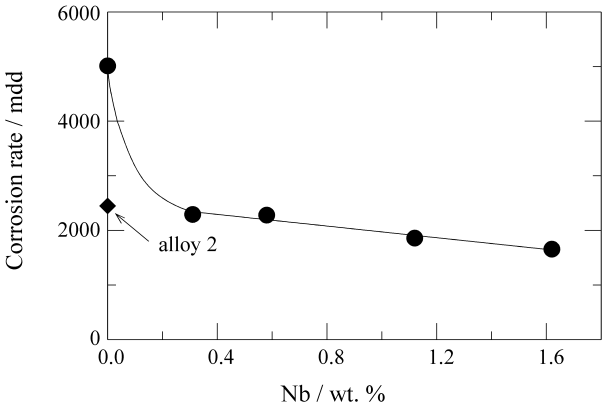

Figure 3. Effect of Nb content upon corrosion rate in 0.5 M H_2SO_4 during the first corrosion step.

Table 2. Slopes of straight lines observed on log-log graphs with the respective time range where they hold and the correlation index r^2.

Alloy	Stage I (min)	Slope	r^2	Stage II (min)	Slope	r^2
1	$10 \le t \le 90$	1.215	0.9938	$90 \le t \le 480$	1.516	0.9949
2	$10 \le t \le 480$	1.044	0.9969	-	-	-
3	$10 \le t \le 60$	1.089	0.9828	$60 \le t \le 240$	1.549	0.9994
4	$10 \le t \le 60$	0.979	0.9909	$60 \le t \le 480$	1.584	0.9977
5	$10 \le t \le 50$	1.006	0.9972	$50 \le t \le 480$	1.609	0.9983
6	$10 \le t \le 60$	0.946	0.9933	$60 \le t \le 480$	1.676	0.9962

$$\Delta m = k\, t^n \quad (1)$$

where Δm is the weight loss, k is a constant, t is the time and n is the slope of the straight line on the log-log graph. The time derivative of this equation indicates that the corrosion rate continually increases with time, and this does not completely agree with the slowing down of the weigh loss increase observed for Nb bearing alloys for times between 240 min and 400 min (see Fig. 1). The reason for this discrepancy is that Eq. 1 is based on data taken from a log-log graph, on which small fluctuations become attenuated. Nevertheless, the conclusions taken from this equation are valid in the sense that on average the corrosion rate continuously increases with time, no matter if during some time intervals it slows down.

3.2. Corrosion potential measurements

The results of corrosion potential variation with time for all six alloys are presented on Fig. 4. After an initial drop the corrosion potential gradually increases with testing time, but it is worth noting that for Nb bearing alloys (alloys 3 to 6) this increase is considerably more intense than for alloys 1 and 2. Another point that has to be emphasized is that the initial corrosion potential of alloy 2 is considerably higher than that of other alloys.

3.3. Corrosion morphology and microconstituents identification

As the corrosion in 0.5M H_2SO_4 solution proceeds the surface of testing samples becomes gradually and uniformly covered with a dark gray corrosion product. As can be observed on Fig. 5 the amount of this product varies with the alloy, being larger on Nb bearing alloys (alloys 3 to 6) and increasing with Nb content. On Mo bearing alloy (alloy 2) the amount of corrosion product is very small.

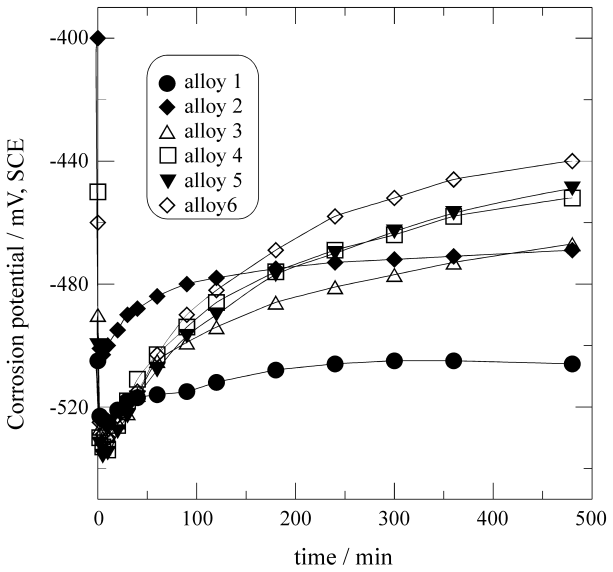

Figure 4. Corrosion potential as a function of time for alloys 1 to 6 in 0.5 M H_2SO_4.

The corrosion product has the consistence of a thin powder and is easily removed from the sample's surface with a cotton pad. After its removal, the metallic surface of all specimens displays a metallographic etching type uniformly corroded surface.

The surface of specimens 1, 2 and 5 was analyzed by energy dispersion (EDS) under three different conditions (as removed from the testing solution, after removal of the corrosion product and after grinding with 600 grit emery paper). It was found that the main elements in the corrosion product of these samples are: alloy 1 - S, P, Cr and Ni; alloy 2 - Cr and Mo; alloy 5 - Nb.

After the removal of corrosion product the morphology of the corroded surface of samples 1, 2 and 5 was examined and its main constituents identified. Figure 6 through 8 show their surface after 150 min testing.

- Alloy 1 (Fig. 6): This alloy shows recrystallized ferrite grains with many inclusions and a continuous precipitate at the grain boundary, probably Cr carbonitrides, as this precipitate is rich in Cr. Most of the inclusions were identified as Si and Al oxides and Mn sulfide. It was found that in 0.5 M H_2SO_4 solution the MnS inclusions are dissolved preferentially to the matrix.
- Alloy 2 (Fig. 7): Its microstructure is similar to that of alloy 2. The continuous precipitate at the grain boundary besides being rich in Cr has also Mo (probably Cr and Mo carbonitrides). The inclusions were identified as Si and Al oxides and no Mn sulfides were found in this alloy, probably due to its low Mn content. In some of the analyzed precipitates the S is bonded to Cr.
- Alloy 5 (Fig. 8): This alloy as well as other Nb bearing alloys is made of recrystallized ferrite grains with precipitates around inclusions and inside the grains. The inclusions contain mostly Al and sometimes Nb sulfide,

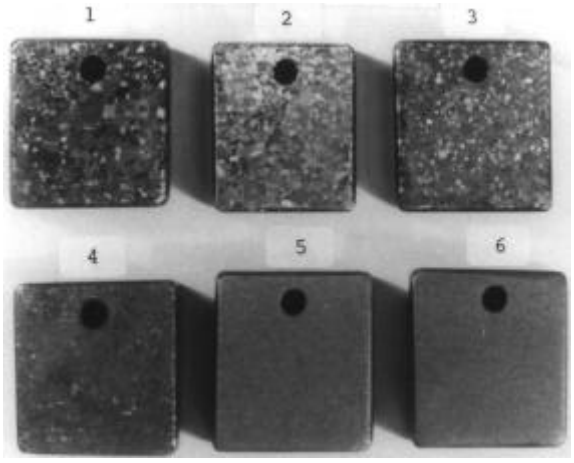

Figure 5. Appearance of samples 1 to 6 after 480 min testing in 0.5 M H_2SO_4. The samples are covered with a corrosion product whose amount increases with Nb content.

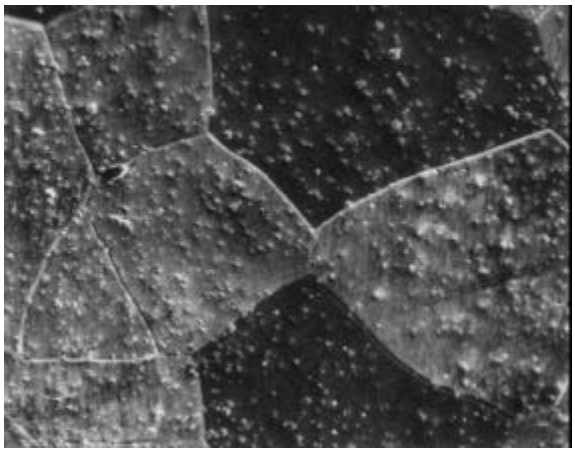

Figure 6. Corroded surface of alloy 1 after 150 min test in 0.5 M H_2SO_4. Ferrite grains with many inclusions and a continuous precipitate at the grain boundary. The observed cavities were formed by selective dissolution of MnS inclusions. SEM. 100X.

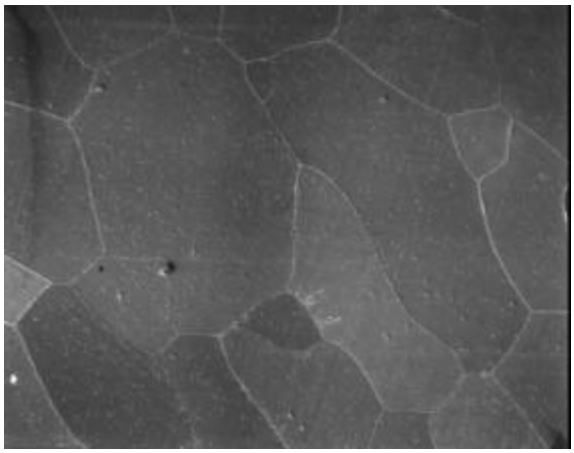

Figure 7. Corroded surface of alloy 2 after 150 min test in 0.5 M H_2SO_4. Ferrite grains with many inclusions and a continuous precipitate at the grain boundary. SEM. 100X.

while the precipitate formed around them is the Fe_2Nb intermetallic compound. The grain boundaries of these alloys are precipitates free and this is a consequence of C and N stabilization with Nb, forming small carbides and nitrides precipitated inside the grains.

4. Discussion

The weight loss tests indicated that with the exception of Mo bearing alloy (alloy 2) the corrosion of the other alloys in 0.5 M H_2SO_4 solution during the initial 480 min testing is a two step process. Thus, each step will be discussed separately.

4.1 First corrosion step

The initial step in the corrosion of a passive alloy is the dissolution of the passive film, so that there is a decrease in corrosion potential due to the gradual increase of active areas on the surface of metal. This was in fact observed

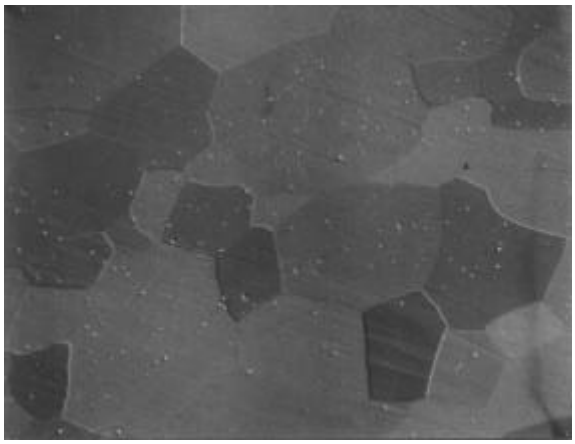

Figure 8. Corroded surface of alloy 5 after 150 min test in 0.5 M H_2SO_4. Ferrite grains with Fe_2Nb intermetallic precipitates around inclusions. SEM. 100X.

during the first 5 to 10 min testing (Fig. 4), suggesting that after this time no passive film is left and only direct metal dissolution is the operative corrosion process.

As observed on Fig. 3 during the first step Nb additions to the ferritic stainless steel decrease the corrosion rate by a factor of more than two. This can be attributed to microstructural alterations that Nb determines inside the alloy and to its own electrochemical features.

In terms of microstructure while the Nb free alloy (alloy 1) presents Cr carbonitrides and manganese sulfide, silica and alumina inclusions, the Nb bearing alloys present Nb carbonitrides and Si or Al oxide inclusions associated to a Nb sulfide and Fe_2Nb precipitates. However, it appears that the main constituent responsible for the larger corrosion rate of the Nb free alloy is the manganese sulfide, and this is supported by the corrosion morphology observed on Fig. 6. The inclusions of this sulfide are attacked by 0.5M H_2SO_4 solution and according to Henthorne[20] in acid solutions the dissolution products of metallic sulfides may stimulate anodic dissolution. On the other hand, Nb combines with S next to the Si or Al oxide inclusions, and the Nb sulfides do not dissolve as the Mn sulfides do. As pointed out by Sedriks[21] Nb_4S_7 is insoluble in acids.

In electrochemical terms Nb could decrease the exchange current density (i_o) of hydrogen reduction reaction over the alloy, and in this way increase the polarization of cathodic reaction which, on its turn, would decrease the corrosion rate. This in fact is feasible as the i_o value[22] for this reaction over Nb in 1 M HCl at 20 °C is only 10^{-11} A/cm^2, while over Fe in the same solution at 10 °C it is 10^{-6} A/cm^2. It should be expected that Nb either in solid solution in Fe or in the intermetallic compound Fe_2Nb would decrease the i_o value, the effect being more pronounced the larger the Nb content.

The mechanism through which Mo increases the corrosion resistance of ferritic stainless steels seems to be different from that proposed for Nb, because its effect on the

microstructure of the alloy is not very sensitive and its i_o value for the hydrogen reaction is very close to that of Fe. In 1 M H_2SO_4 this value[23] is 10^{-6} A/cm^2. Several authors[24-27] suggest that a layer of Mo ion compounds is formed on the metal surface, acting as a barrier against the electrochemical attack. Rhodin[24], for instance, based on its experimental results, concluded that Mo forms on metal surface amorphous and insoluble acid compounds that protect the material against further attack. Although most of these works are concerned with pitting corrosion, the proposed mechanism seems to be suitable also for generalized corrosion in acid solutions.

4.2 Second corrosion step

In acid solutions the corrosion rate increase that is observed in weight loss tests after certain time is usually due to the increase of the exposed area because the surface becomes rough. Here this is not the case as the specimens maintain during this step their surface smooth and free from any significant irregularity.

The reason for the observed behavior must be associated to the corrosion product that is formed on the surface of the sample. This product becomes perceptible only when the second step takes over.

On Nb bearing alloys (alloys 3 to 6) the corrosion product would have a double effect: (1) it increases the corrosion rate through the depolarization of cathodic reaction, and (2) it decreases the corrosion rate through polarization increase of anodic reaction. The first effect is based on the fact that both the corrosion potential and the corrosion rate increase simultaneously with time. The second effect is a consequence of the protection delivered by the corrosion product, which makes the electrolyte access to the metal difficult, that is, it decreases the exposed area and this implies in a polarization increase of the anodic curve.

For times between 60 and 180 min both the corrosion potential and the corrosion rate of alloys 3 to 6 increase with time. During this period the depolarization of cathodic curve is predominant. After 180 min the corrosion potential continues to increase but the corrosion rate comes to a standstill or even decreases and this means that the polarization increase of anodic curve becomes predominant. This predominance lasts to about 300 min when again the cathodic depolarization takes over increasing both the corrosion rate and the corrosion potential. The protective effect of corrosion product formed seems to be porosity dependant and after 300 min, no matter how much product is formed on the surface, the protection given is very little affected as it becomes controlled almost exclusively by the porosity. It appears that at this point the porosity attains a value that is practically unaffected by the amount of corrosion product present on the surface.

The amount of corrosion product formed on Nb free alloy (alloy 1) is considerably smaller than on Nb bearing alloys, and this explains why it attains higher corrosion rates since the protection given by this product is also smaller and is less effective in counteract the cathodic depolarization. The small variation of corrosion potential of this alloy is consistent with the smaller amount of corrosion product because in this way the anodic curve is very little affected.

The distinct behavior of Mo bearing alloy 2 is certainly associated to the small amount of corrosion product formed on its surface as well as to its higher initial corrosion potential. It may be assumed that this product is insoluble and that it inhibits the electrochemical dissolution in a way similar to that proposed by several authors[24-27] for pitting corrosion.

4.3 Cathodic depolarization

The cathodic depolarization, to which the corrosion rate increase with time is attributed, seems to be related to the chemical composition of corrosion product formed. There is the possibility of the hydrogen overpotential of this product being small and this would account for the assumed cathodic depolarization. Takamura *et al.*[28] suggested that the corrosion rate could be changed by the accumulation of alloy elements on the surface, both in metallic form and as a compound, each one affecting in a certain way the hydrogen overpotential. The accumulation of Nb on the surface during active dissolution of ferritic steel in sulfuric acid solution was experimentally confirmed by Seo *et al.*[17]. Uhlig[29] and Takamura *et al.*[28] suggest that S and P, precipitated in steels as sulfides and phosphides, lower the hydrogen overpotential. This probably accounts for the cathodic depolarization on alloy 1 whose corrosion product contains these elements. On the corrosion product formed on Nb bearing alloys these elements are absent and in this case the depolarization has to be credited to a Nb containing compound, probably a niobium oxide, and to the enrichment of the steel surface with Nb.

5. Conclusions

The addition of Nb to a 17% Cr ferritic stainless steel in amounts larger than that necessary to stabilize the interstitial elements affects considerably its corrosion behavior in a 0.5 M H_2SO_4 solution. While for a Mo bearing alloy the corrosion rate is constant with time, for Nb bearing alloys, after an initial stage of about 60 min, this rate changes with time. The reasons for this change are probably associated with the corrosion product formed on the surface and the enrichment of the steel surface with Nb, both of which seems to affect the overpotential of both anodic and cathodic reactions. The amount of corrosion product increases with Nb content and appears to be formed almost exclusively by Nb compounds.

In present investigation it became evident that the evaluation of corrosion behavior of a material cannot be

performed through short duration tests. Even a 480 min (8 h) test that was carried out in present work was not conclusive as to the long term behavior of investigated alloys.

Acknowledgments

The authors are indebted to Companhia Brasileira de Metalurgia e Mineração - CBMM for financial support of this work and to Instituto de Pesquisas Tecnológicas do Estado de São Paulo S.A. - IPT for the use of its laboratories and equipment.

References

1. Truman, J.E.; Crawshaw, B. *Proceedings of Conference on Stainless Steel for the Fabricator and User*, Birmingham, England, p. 195-204, 1968.
2. Dundas, H.J.; Bond, A.P. *Intergranular Corrosion of Stainless Alloys*, ed. Steigerwald, R.F.; ASTM, Philadelphia, PA, USA, p. 154-178, 1978.
3. Cowan II, R.L.; Tedmon Jr., C.S. *Corrosion Science and Technology*, eds. Fontana, M.G.; Staehle, R.W. Plenum Press, New York, NY, USA, p. 293-400, 1973.
4. Pickering, F.B. *Intern. Met. Rev.*, v. 21, p. 227-268, 1976.
5. Demo, J.J.; Bond, A.P. *Corrosion*, v. 31, n. 1, p. 21-22, 1975.
6. Steigerwald, R.F.; Dundas, H.J.; Redmond, J.D.; Davison, R.M. *Stainless Steel'77*, Climax Molybdenum Company, London, England, p. 57-72, 1977.
7. Bond, A.P. *Trans. Met. Soc. AIME*, v. 245, p. 2127-2134, 1969.
8. Abo, H.; Nakazawa, T.; Takemura, S.; Onoyama, M.; Ogawa, H.; Okada, H. *Stainless Steel'77*, Climax Molybdenum Company, London, England, p. 35-47, 1977.
9. Bond, A.P.; Lizlovs, E.A. *J. Electrochem. Soc.*, v. 116, n. 9, p. 1305-1311, 1969.
10. McKee, I.J.; Jackson, R. *Proceedings of 6th International Congress on Metallic Corrosion*, Sydney, Australia, v. 2, p. 1620-1637, 1975.
11. Davis, J.A.; Deverell, H.E.; Nichol, T.J. *Corrosion*, v. 36, n. 5, p. 215-220, 1980.
12. Demo, J.J. *Handbook of Stainless Steels*, eds. Peckner, D.; Bernstein, I.M. McGraw-Hill, New York, NY, USA, p. 5-1 - 5-40, 1977.
13. Streicher, M.A. *Corrosion*, v. 30, n. 3, p. 77-91, 1974.
14. Maximovitch, S.; Barral, G.; Le Cras, F.; Claudet, F. *Corrosion Science*, v. 37, n. 2, p. 271-291, 1995.
15. Seo, M.; Guo, J.; Hultquist, G.; Leygraf, C.; Sato, N. *Key Engineering Materials*, v. 20-28, p. 271-278, 1988.
16. Guo, J.; Seo, M.; Sato, Y.; Hultquist, G.; Leygraf, C.; Sato, N. *Boshoku Gijutsu*, v. 35, n. 5, p. 283-288, 1986.
17. Seo, M.; Hultquist, G.; Leygraf, C.; Sato, N. *Corrosion Science*, v. 26, n. 11, p. 949-960, 1986.
18. Davies, R.D. *Corrosion*, v. 49, n. 7, p. 544-549, 1993.
19. Potgieter, J.H. *Journal of Materials Science Letters*, v. 15, n. 16, p. 1408-1411, 1996.
20. Henthorne, M. *Corrosion*, v. 26, n. 12, p. 511-528, 1970.
21. Sedriks, A.J. *Intern. Met. Rev.*, v. 28, n. 5, p. 295-307, 1983.
22. Shreir, L.L. *Corrosion*, John Wiley, New York, NY, USA, v. 2, p. 21-30, 1963.
23. Conway, B.E. *Electrochemical Data*, Elsevier, New York, NY, USA, p. 335-359, 1952.
24. Rhodin, T.N. *Corrosion*, v. 12, n. 9, p. 55-65, 1956.
25. Ogura, K.; Ohama, T. *Corrosion*, v. 40, n. 2, p. 47-51, 1984.
26. Kodama, T.; Ambrose, J.R. *Corrosion*, v. 33, n. 5, p. 155-161, 1977.
27. Ambrose, J.R. *Corrosion*, v. 34, n. 1, p. 27-31, 1978.
28. Takamura, A.; Shimogori, K.; Arakawa, A. *Proceedings of 4th International Congress on Metallic Corrosion*, Houston, TX, USA, p. 466-472, 1972.
29. Uhlig, H.H. *Corrosion and Corrosion Control*, John Wiley, New York, NY, USA, p. 45-49 and 106-108, 1963.